Australian Meteorological and Oceanographic Journal 63 (2013) 443–456

Seasonal climate summary southern hemisphere (summer 2012–13): Australia's hottest summer on record and extreme east coast rainfall

Christopher J. White[1,2] and Paul Fox-Hughes[3,4]
[1]Centre for Australian Weather and Climate Research (CAWCR),
Bureau of Meteorology, Australia
[2]School of Engineering and ICT, University of Tasmania, Australia
[3]Tasmania and Antarctica Region, Bureau of Meteorology, Australia
[4]Antarctic Climate and Ecosystems Cooperative Research Centre, Australia

(Manuscript received July 2013; revised February 2014)

Southern hemisphere circulation patterns and associated anomalies for austral summer 2012–13 are reviewed, with an emphasis on Pacific Basin climate indicators and Australian rainfall and temperature. Summer 2012–13 was a neutral ENSO period but saw an active burst of the Madden-Julian oscillation in January and February. The summer saw record-breaking temperatures across the country, with a widespread and persistent heatwave in January affecting all States and Territories and contributing to the warmest summer on record for Australia as a whole. Summer rainfall was below average Australia-wide, however extreme rainfall from tropical cyclone *Oswald* caused widespread record flooding in eastern Queensland and New South Wales at the end of January. In contrast, rainfall was below average in central and northern regions, particularly in the Northern Territory, due to the late onset of a weak Australian monsoon.

Introduction

This summary reviews the southern hemisphere and equatorial climate patterns for summer 2012–13, with particular attention given to the Australasian and Pacific regions. The main sources of information for this report are analyses prepared by the Bureau of Meteorology's National Climate Centre and the Centre for Australian Weather and Climate Research (CAWCR).

Pacific Basin climate indices

Southern Oscillation Index

The Troup Southern Oscillation Index[1] (SOI) is based on the mean sea-level pressure (MSLP) difference between Tahiti and Darwin, where sustained negative values below –8 generally indicate an El Niño event, while sustained positive values above +8 are associated with La Niña periods. Figure 1 shows monthly SOI values from January 2009 to February 2013, together with a five-month weighted moving average.

In contrast to the two previous summers of 2010–11 (Imielska 2011) and 2011–12 (Webb 2012), which attained exceptional monthly SOI values coinciding with the peaks of two strong consecutive La Niña events, values of the SOI were predominantly neutral to moderately negative throughout 2012 (Fig. 1). SOI values peaked in June 2012 with a negative value of –10.4. From July 2012, SOI values continued in a neutral phase, oscillating between slightly positive and negative values, leading to overall negative summer 2012–13 values of –6.0 (December), –1.1 (January) and –3.6 (February), with an average summer value of –3.58.

Monthly mean sea level pressure (MSLP) was close to or below average at both Darwin and Tahiti during summer 2012–13. MSLP anomalies for Darwin, relative to a 1933–1992 climatology, were slightly positive in December, moving to slightly negative in January and then returning to slightly

[1]The Troup Southern Oscillation Index (Troup 1965) used in this article is ten times the standardised monthly anomaly of the difference in mean sea level pressure (MSLP) between Tahiti and Darwin. The calculation is based on a sixty-year climatology (1933–1992). The Darwin MSLP is provided by the Bureau of Meteorology, and the Tahiti MSLP is provided by Météo France inter-regional direction for French Polynesia.

Corresponding author address: Christopher White, CAWCR, Bureau of Meteorology, GPO Box 1289, Melbourne Vic. 3001, Australia.

Fig. 1. Southern Oscillation Index, from January 2009 to February 2013, together with a five-month binomially weighted moving average. Means and standard deviations used in the computation of the SOI are based on the period 1933–1992.

Fig. 2. 5VAR composite standardised monthly ENSO index from January 2009 to February 2013, together with a weighted three-month moving average. See text for details.

positive again in February. MSLP anomalies were negative at Tahiti throughout the summer, although anomalies were generally weak, indicating that Tahiti's MSLP had a marginally greater influence on the negative SOI values than Darwin. Monthly MSLP anomalies for Darwin were +0.3, –0.6 and +0.7 hPa for December, January and February respectively, and at Tahiti were –0.9, –0.9 and –0.1 hPa (not shown).

Composite multivariate ENSO indices

Composite multivariate El Niño–Southern Oscillation (ENSO) indices are often regarded as more complete indicators of ENSO activity than those based solely on one variable, such as MSLP or sea surface temperature (SST), as they bring several atmospheric and oceanic parameters together.

The 5VAR[2] index is one such multivariate ENSO index (Kuleshov et al. 2009), calculated as the standardised amplitude of the first principal component of monthly Darwin and Tahiti MSLP[3] and monthly NINO3, NINO3.4 and NINO4 SST[4]. Following two years of negative 5VAR values associated with the 2010–11 and 2011–12 La Niña events (Fig. 2), 5VAR values rose through autumn (Martin 2013) and winter (Pepler 2013) 2012, peaking in August with a moderate value of +1.0. The 5VAR values then fell, reaching and maintaining slightly negative neutral values throughout summer 2012–13 of –0.12, –0.15 and –0.12 for December, January and February respectively, with an overall summer average of –0.13.

Another multivariate index is the US Climate Diagnostics Center's Multivariate ENSO Index (MEI)[5], which is derived from a number of atmospheric and oceanic parameters, calculated as a two-month mean and where large negative (positive) anomalies are usually associated with La Niña (El Niño) events. The December–January (+0.042) and January–February (–0.163) MEI values show a slight decreasing trend following a peak in June–July 2012 of +1.139 (not shown), similar to that of the 5VAR index (Fig. 2) and consistent with neutral ENSO conditions.

Outgoing long-wave radiation

Outgoing long-wave radiation (OLR) over the equatorial Pacific Ocean is a good proxy of deep convection in the tropics, with decreases in OLR associated with increases in convection, and vice versa. Convection in the equatorial region, centred about the Date Line, is sensitive to changes in the Walker Circulation. Studies such as Hoerling et al. (1997) have shown that during La Niña events, OLR is generally increased (that is, convection is suppressed) along the equator, particularly along the equator near and west of the Date Line. During El Niño events the opposite is generally true with OLR typically reduced (that is, convection is enhanced), particularly near and east of the Date Line.

Standardised monthly anomalies[6] of OLR are computed by the Climate Prediction Center, Washington, over the equatorial Pacific region near the Date Line, ranging from 5°S to 5°N and 160°E to 160°W. Monthly standardised OLR anomalies for summer 2012–13 were +0.7, –0.2 and +0.1 for December, January and February respectively. This shows that convection was initially suppressed over this area in December but was near-neutral in January and February consistent with neutral ENSO conditions indicated by the

[2]ENSO 5VAR was developed at the Bureau's National Climate Centre and is described in Kuleshov et al. 2009. The principal component analysis and standardisation of this ENSO index is performed over the period 1950–1999.
[3]MSLP data obtained from www.bom.gov.au/climate/current/soihtm1.shtml. As previously mentioned, the Tahiti MSLP data are provided by Météo France inter-regional direction for French Polynesia.
[4]SST indices obtained from ftp://ftp.cpc.ncep.noaa.gov/wd52dg/data/indices/sstoi.indices

[5]Multivariate ENSO Index obtained from www.esrl.noaa.gov/psd/people/klaus.wolter/MEI/table.html. The MEI is a standardised anomaly index described in Wolter and Timlin (1993, 1998).
[6]Standardised monthly OLR anomalies are obtained from www.cpc.ncep.noaa.gov/data/indices/olr

Fig. 3. OLR anomalies for summer 2012–13 (W m^{-2}) with respect to a base period of 1979–2000. The mapped region extends from 40°S to 40°N and from 70°E to 180°E.

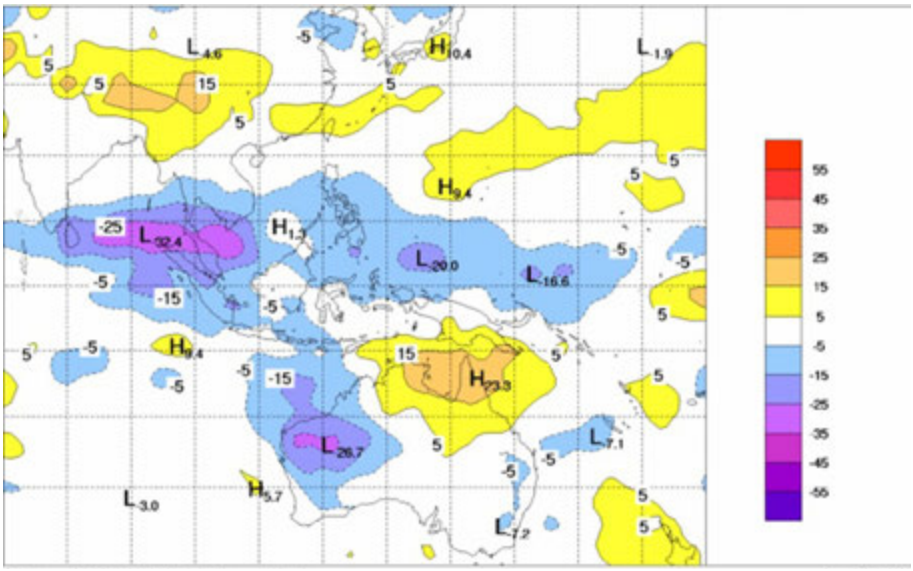

Fig. 4. Phase-space representation of the MJO index (Wheeler and Hendon 2004) for summer 2012–13. Daily values are shown with December in green, January in blue and February in red. The eight MJO phases and corresponding approximate locations of the near-equatorial enhanced convective signal are labelled. Strong MJO activity is associated with daily values outside the unit circle.

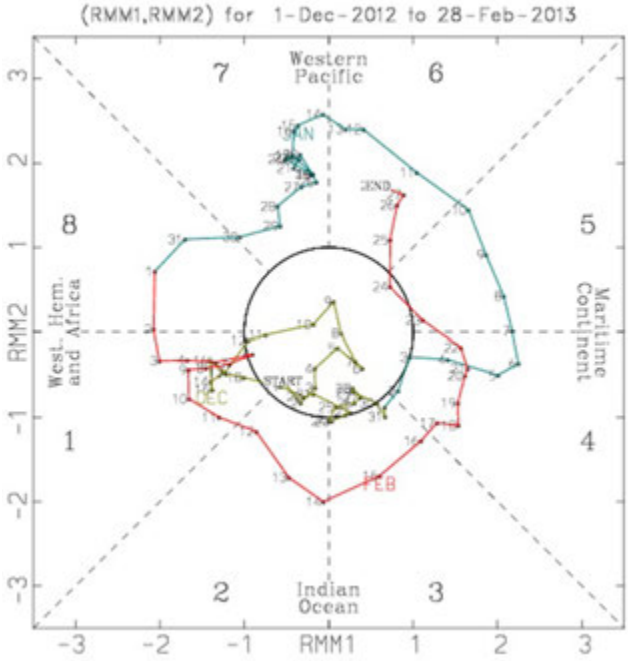

5VAR index above.

Figure 3 shows the spatial pattern of seasonal OLR anomalies across the Asia-Pacific tropics for summer 2012–13. Strongly negative OLR anomalies were evident over much of Western Australia during the summer, and, to a lesser degree, a small area over eastern Australia. This

Fig. 5. Time-longitude section of daily-averaged OLR anomalies, averaged for 15°S to 15°N, for the period October 2012 through to February 2013. Anomalies are with respect to a base period of 1979–2010.

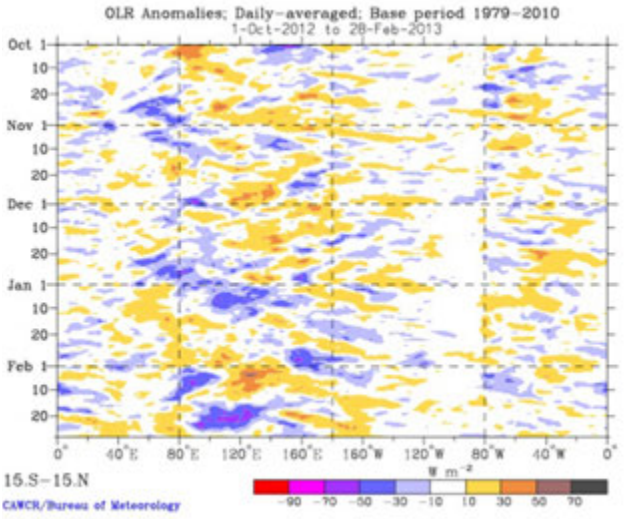

was correlated with above average to very much above average rainfall deciles across northwestern Western Australia (discussed later). In contrast, an area of positive OLR anomalies extended over northern Queensland and the Northern Territory during the summer, associated with average to below average rainfall deciles in this region (also discussed later). Weak positive OLR anomalies were evident along the equator between 160°E and 180°E, consistent with the monthly standardised anomalies discussed above. Similarly, strong negative OLR anomalies in the eastern Indian Ocean were analogous with a continued decline in the positive phase of the Indian Ocean Dipole that peaked in September 2012 (Reid 2013).

Fig. 6. SST anomalies for summer 2012–13 (°C).

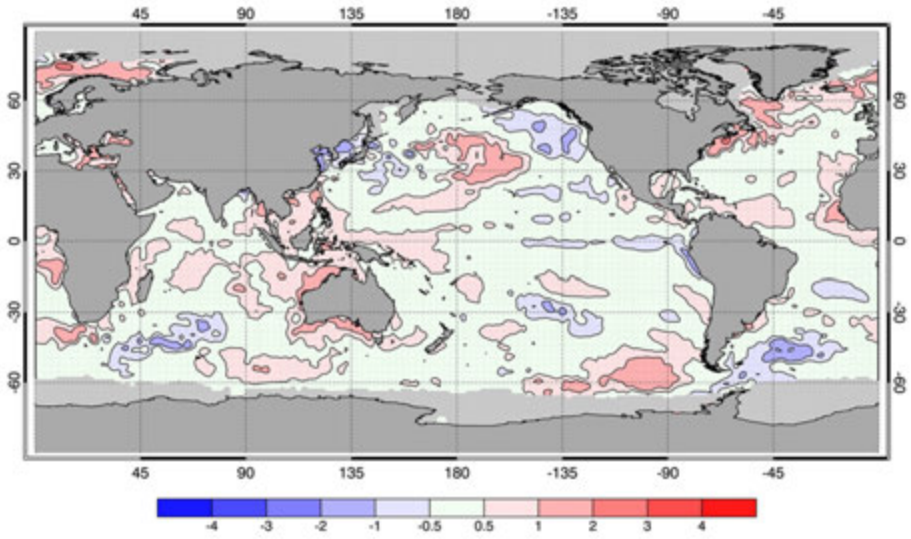

Madden-Julian Oscillation

The Madden-Julian Oscillation (MJO) is an important driver of atmospheric variability on the intra-seasonal timescale. When strong, the MJO is visible as a tropical atmospheric anomaly that develops in the Indian Ocean and propagates eastwards into the Pacific Ocean (Zhang 2005, Donald et al. 2006), taking approximately 30 to 60 days to reach the western Pacific and with a frequency of six to twelve events per year. During austral summer, the convective variability of the MJO is typically strongest in the northern hemisphere and impacts over Australia are generally weakened (e.g. Wheeler et al. 2009). A description of the real-time Multivariate MJO (RMM) index and the associated phases can be found in Wheeler and Hendon (2004). The phase-space diagram of the RMM index for summer 2012–13 is shown in Fig. 4, with the evolution of tropical OLR convection anomalies along the equator shown in Fig. 5.

The MJO was active for much of summer 2012–13. The MJO showed some activity in the middle of December (phase one) but weakened after a few days of activity. It remained largely inactive until the end of December where it started to show some activity in the Indian Ocean (phase three). However, it was not until 4 January that there was a burst of activity as the MJO strengthened and moved eastwards through the Maritime Continent (phases four and five) and into the Western Pacific (phases six and seven), peaking on 14 January[7]. The MJO decreased in strength as it progressed through the Western Pacific (phase seven) in the second half of January before strengthening again between 29 January and 3 February as it entered the western hemisphere (phase eight into phase one). The MJO then weakened for the next week (phase one), but became more active again from 7 February and remained active as it moved through phases one to four until 22 February. As it entered phase five on 23 February, it weakened before increasing in strength again in the Western Pacific after 25 February (phase six). The MJO remained active at the end of February.

The progress of the MJO through summer 2012–13 can also be tracked in the OLR anomaly time-longitude section (Fig. 5). The negative OLR anomalies from late December and into January between approximately 50°E and the Date Line correspond with the first active burst of the MJO as it moved from the Indian Ocean across the Maritime Continent and into the Western Pacific. The second burst of the MJO can be seen in the negative OLR anomalies between approximately 80°E and 160°E in February as it moved through the western hemisphere, the Indian Ocean and into the Maritime Continent.

Oceanic patterns

Sea-surface temperatures

Global SST anomalies for summer 2012–13 are shown in Fig. 6. In the equatorial Pacific Ocean, weak negative anomalies in the east and warm anomalies further west are suggestive of a La Niña pattern, but are not sufficiently strong to represent a clear signal of anything but neutral conditions, which is analogous with the 5VAR index (Fig. 2) for the season. Elsewhere in the Pacific, anomalies are largely positive, apart from a broad ring around the coastal north Pacific and a band of generally negative weak anomalies across the central south Pacific near 30°S.

SSTs in the tropical Indian Ocean were uniformly positive. The only significant area of negative anomaly in the Indian Ocean as a whole was to be found south of about 30°S between roughly 45°E and 85°E. The North Atlantic Ocean was again very largely characterised by anomalous warmth, particularly in areas of the far north. Sea surface

[7]The amplitude of the MJO is measured by $(RMM1^2 + RMM2^2)^{1/2}$, where RMM1 and RMM2 are described by Wheeler and Hendon (2004). Records began in June 1974.

Fig. 7. Time-longitude section of the monthly anomalous depth of the 20 °C isotherm at the equator (2°S to 2°N) for January 2009 to February 2013. (Plot obtained from the TAO Project Office)

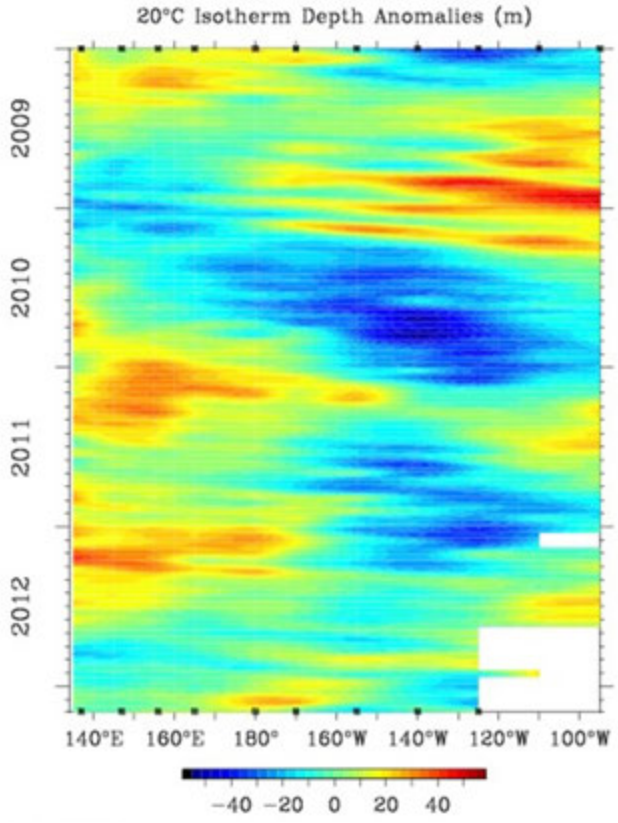

temperature anomalies in the vicinity of Australia were generally positive. In particular, near-coastal waters off the northwest and southern coasts experienced anomalies of +2 to +3 °C during the summer.

Subsurface patterns

The 20 °C isotherm along the equator (2°S to 2°N) corresponds well with the depth of the equatorial thermocline separating warm surface water from colder deep ocean water. Anomalies in the depth of the 20 °C isotherm indicate the presence of warmer (greater depth) or colder (lesser depth) water than is normal. These indicators can be a useful guide to subsequent changes in corresponding SSTs, pointing, for example, to the presence or potential for upwelling of cold water and to the likelihood of El Niño or La Niña conditions developing.

Figure 7 presents a Hovmöller diagram of the 20 °C isotherm depth anomaly for the period January 2009 to February 2013, using NOAA TAO/TRITON data[8]. The strong La Niña of summer 2010–2011 (Imielska 2011) is clearly evident as a pattern of an anomalously deep 20 °C isotherm in the western Pacific and correspondingly shallow 20 °C isotherm in the eastern equatorial Pacific. Similarly, a weaker

[8]Hovmöller plot obtained from www.pmel.noaa.gov/tao/jsdisplay/

Fig. 8. Four-month November 2012 to February 2013 sequence of vertical sea subsurface temperature anomalies at the equator for the Pacific Ocean. The contour interval is 0.5 °C. (Plot obtained from CAWCR).

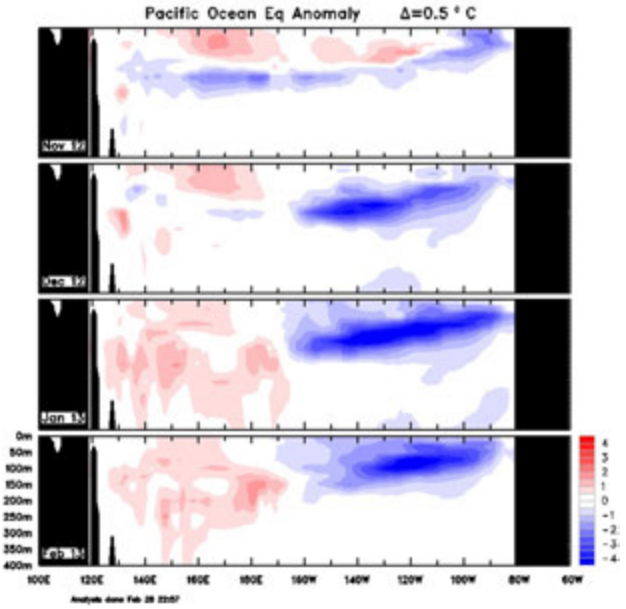

La Niña is discernable during the summer of 2011–2012 (Webb 2012). By the end of autumn 2012 La Niña conditions had dissipated (Martin 2013) and summer 2012–13 saw a continuation of the neutral conditions that had dominated the equatorial Pacific since mid-2012 (Pepler 2013, Reid 2013), with no region of broadscale up- or down-welling evident.

Monthly cross-sections of equatorial Pacific sea temperatures between November 2012 and February 2013 (Fig. 8) show the development in December of a pool of subsurface cold water east of the date line. The cold pool expanded and intensified somewhat in December, approaching the surface of the equatorial eastern Pacific before weakening in February. Conditions in the western Pacific were generally weakly warmer than normal during summer 2012–13.

Atmospheric patterns

Surface analyses

The southern hemisphere MSLP pattern for summer 2012–13 is given in Fig. 9, with the corresponding anomaly pattern in Fig. 10, the latter having been calculated from a 1979–2000 base climatology. Grey shading in Fig. 10 represents elevated areas, for which MSLP anomalies have not been calculated. At mid-latitudes, during summer 2012–13 the subtropical ridge was interrupted only by the presence of the continental landmasses of Australia, Africa and, particularly, South America, as is climatologically normal for the time of year. High pressure centres were located in the east Pacific near 100°W, central Atlantic near 15°W and Indian Ocean near 90°E. The subtropical ridge was, in fact, close to its

Fig. 9. Summer 2012–13 MSLP (hPa). The contour interval is 5 hPa.

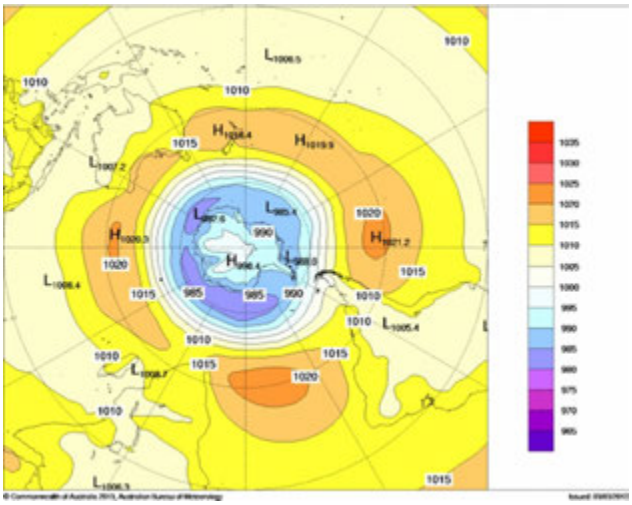

Fig. 10. Summer 2012–13 MSLP anomalies (hPa), from a 1979–2000 climatology.

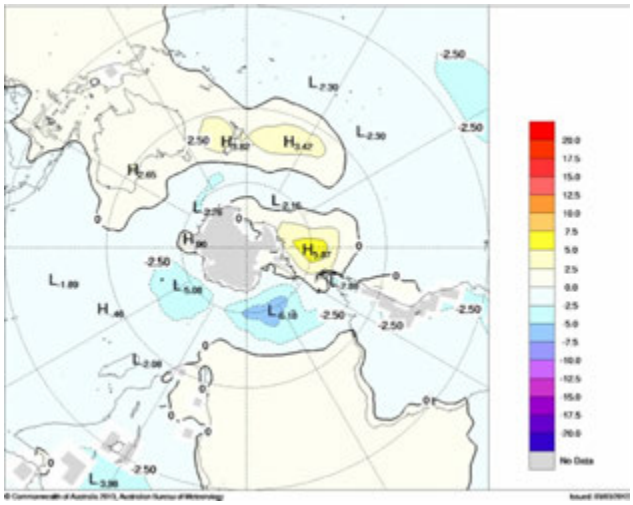

Fig. 11. Summer 2012–13 500 hPa mean geopotential height (gpm).

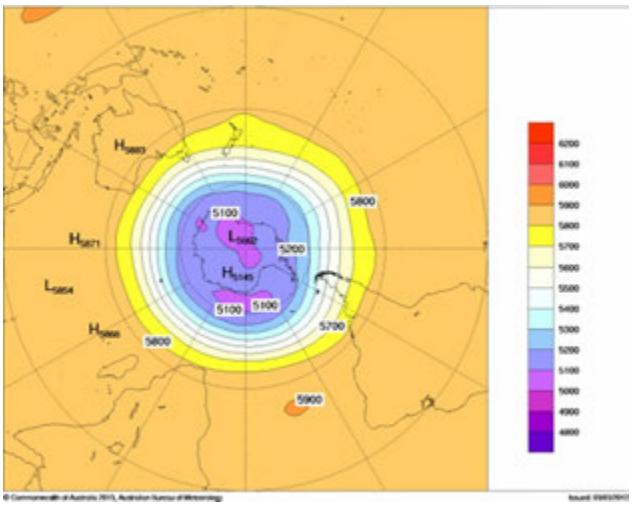

Fig. 12. Summer 2012–13 500 hPa mean geopotential height anomalies (gpm), from a 1979–2000 climatology.

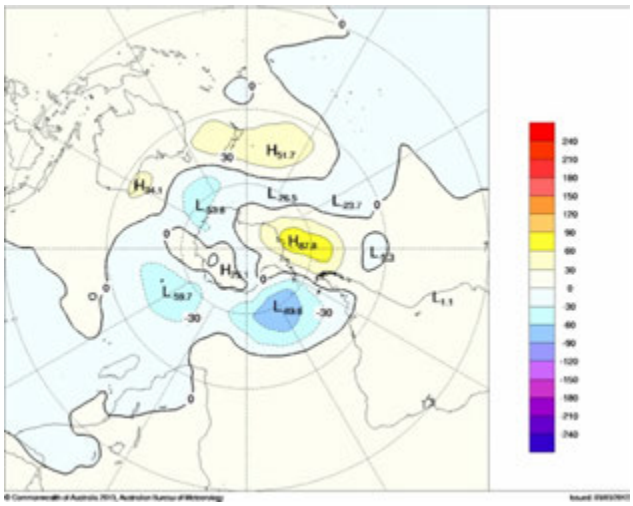

climatological norm, with higher than average pressure only immediately to the west and east of New Zealand (Fig. 10). The circumpolar trough was characterised by deeper than average low centres of 985 hPa near 0°E and 45°E, representing anomalies of –6.18 and –5.08 hPa respectively. Near 90°W, west of Drake Passage, the circumpolar trough was weaker than normal, with an MSLP anomaly of +5.87 hPa.

The lack of a strong pattern in the three-monthly mean and anomaly charts is due largely to a switch between SAM modes during the period (discussed below). In December, anomalous high pressure ringed the Antarctic continent, with anomalous low pressure to the north (not shown). This pattern began to break down in January, and by February had reversed to one of anomalously low circumpolar MSLP with a weaker belt of anomalously high pressure in the mid-latitudes.

Mid-tropospheric analyses

The 500 hPa geopotential height field gives an indication of the steering of mid-latitude surface pressure systems. The mean 500 hPa geopotential height for summer 2012–13 is shown in Fig. 11, with the corresponding anomaly field in Fig. 12. At mid-latitudes, the height field is broadly zonal. Troughs are evident at higher latitudes near 60°E, 120°E, and 130°W, with a broad trough straddling the Greenwich Meridian. Circumpolar anomalies reflect those at the surface (Fig. 10), with negative anomalies near 30°W, 60°E and south of Australia near 135°E, with a strong positive anomaly near 90°W. In the mid-latitudes, the most significant feature of the anomaly field was a positive anomaly to the east of New Zealand near 165°W. The relative positions of this positive anomaly and the negative anomaly to the south of Australia ensured that the 500 hPa pattern was favourable for steering surface synoptic pressure systems in a southeasterly

Fig. 13. Mean southern hemisphere blocking index (BI) anomaly (m s^{-1}) for summer 2012–13 (solid blue line). Dashed blue line shows the corresponding absolute BI (m s^{-1}) for the season. The horizontal axis shows degrees east of the Greenwich meridian. (Plot obtained from CAWCR).

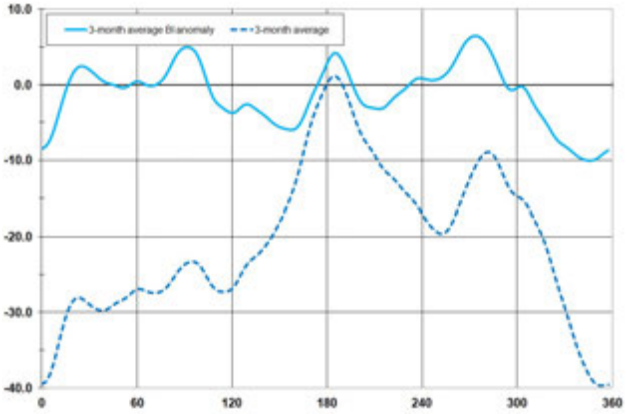

direction over southeastern Australia, thus contributing to a difficult fire weather season in that region.

Southern Annular Mode

The Southern Annular Mode (SAM) or Antarctic Oscillation (AAO) is the approximately meridional (or north–south) oscillation of mass between the southern hemisphere mid-latitudes and polar regions. SAM can be detected through the depth of the troposphere via a number of parameters, including surface pressure. A positive (negative) SAM index corresponds to increased (decreased) air mass over the southern hemisphere mid-latitudes, and decreased (increased) mass over high southern latitudes, with a poleward contraction (equatorward expansion) of mid-latitude westerly winds. The NOAA Climate Prediction Centre routinely monitors the SAM, producing a standardised monthly SAM index[9]. During summer 2012–13, the SAM index switched from a negative to positive phase. In December, the index was –0.76, in January 2013 +0.07 and in February +0.72. The seasonal average value of +0.03 does not, therefore, tell the full story of the index during the summer, however, the change in SAM index as noted above does account for a seasonally weak MSLP anomaly signal.

Blocking

The Tasman Sea and southwest Pacific Ocean to the immediate east of Australia is recognised as the southern hemisphere region most susceptible to the formation of atmospheric blocks (Risbey et al. 2009). These features have a significant impact on southern Australian rainfall. The Blocking Index (BI) is given by:

$$\mathrm{BI} = 0.5\,[(u_{25} + u_{30}) - (u_{40} + 2u_{45} + u_{50}) + (u_{55} + u_{60})]$$

where u_x is the westerly component of the 500 hPa wind at latitude x. BI is an indicator of the relative strength of 500 hPa mid-latitude (40°S to 50°S) westerly flow in comparison to subtropical (25°S to 30°S) and higher latitude (55°S to 60°S) flow. Positive values are most frequently associated with split flow in the mid-latitude westerlies and blocking around 45°S.

Figure 13 shows the BI for each 2.5° longitude interval averaged over the summer 2012–13 period, together with anomalies from the long term mean. Positive BI anomalies are evident in several regions around the globe during this period: between 10°E and 110°E, 170°E and 200°E (160°W), and 230°E (130°W) to 290°E (70°W). However, it was only the second of these for which the BI was positive on average over the southern summer, consistent with evidence of split flow near the date line in the 500 hPa geopotential height anomaly field (Fig. 12).

Winds

Figures 14 and 15 display anomalies from the 22 year NCEP II climatology of 850 hPa and 200 hPa winds over summer 2012–13. Anti-cyclonic anomalies in the 850 hPa plot to the east of New Zealand and west of Drake Passage correspond to anomalies of high pressure in MSLP (Fig. 10). The slight onshore anomaly over the Queensland and northern New South Wales coasts is consistent with the heavy rainfall events experienced in those areas (discussed later). Similarly, an easterly offshore anomaly over northwestern Australia reflects the delayed monsoon that played a prominent role in the extreme temperatures experienced over the continent during the summer (also discussed later). In monthly charts (not shown), a slight westerly anomaly is evident in mid-latitudes and easterly anomaly at higher latitudes, reversing in February, indicative of the switch in SAM mode. In the three-monthly mean chart, however, these influences have largely cancelled each other. Similarly, there is little clear signal evident in the 200 hPa anomaly, consistent with both the switch in SAM mode and the neutral ENSO conditions in the Pacific Ocean (see earlier sections).

Australian region

Rainfall

Rainfall totals (Fig. 16) and deciles (Fig. 17) show that much of southern, central and northern Australia was drier than normal during summer 2012–13, receiving average to below average rainfall, with some areas—notably around Darwin, Kakadu and Arnhem Land in the Northern Territory—seeing very much below average rainfall totals. Conversely, large areas of Western Australia saw above average to very much above average rainfall during the summer. Similarly, coastal and inland regions of eastern Queensland and New South Wales experienced very much above average rainfall totals for the season, produced by very heavy rainfall at the end of January 2013 as a result of the former category 1 tropical cyclone *Oswald* (see Special Climate Statement 44, Bureau of Meteorology 2013a).

[9]For more information on the SAM index from the Climate Prediction Center (NOAA), see www.cpc.ncep.noaa.gov/products/precip/CWlink/daily_ao_index/aao/aao.shtml

Fig. 14. Summer 2012–13 850 hPa vector wind anomalies (m s^{-1}).

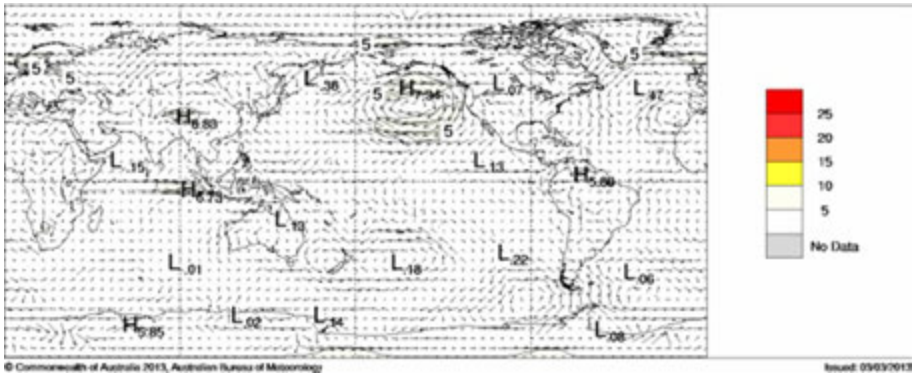

Fig. 15. Summer 2012–13 200 hPa vector wind anomalies (m s^{-1}).

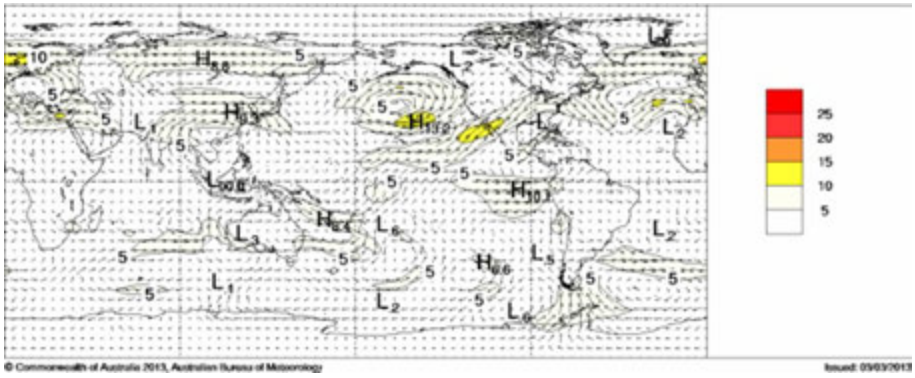

When averaged across Australia, summer 2012–13 rainfall was below average (–13 per cent) and the 36th driest summer from 113 years of record (Table 1). The national area-averaged total for the season was particularly influenced by the significantly drier conditions observed in the north of the country where the highest summer rainfall totals typically occur. The late onset of a weak Australian monsoon—typically the monsoon starts around the last week in December but this season the onset was not until 17 January—influenced the drier than normal summer rainfall totals over much of the Northern Territory. The observed positive OLR anomalies (Fig. 3) provide evidence of the reduced cloudiness in this region. Many sites across the Northern Territory saw their driest December on record, attributable to the lack of monsoon rainfall, which contributed to the 18th driest summer on record. However, the national area-average masks the spatial variance across the country, with South Australia recording below average rainfall of –59 per cent and, conversely, Western Australia receiving above average rainfall of +20 per cent for the summer. All other States and Territories observed below average rainfall totals including Queensland (–20 per cent) and New South Wales (–3 per cent), despite the very much above average rainfall deciles in eastern regions (Fig. 17). The higher than normal rainfall totals evident across much of northwestern Western Australia were correlated with the strongly negative OLR anomalies evident over much of the region (Fig. 3). The influence of ENSO on Australian summer 2012–13 rainfall was minimal, with neutral ENSO conditions reached in spring 2012 following near El Niño conditions in winter (Reid 2013), which were then sustained throughout the summer (Fig. 2).

Several notable heavy rainfall events significantly contributed to the wetter than normal conditions in Western Australia and coastal areas of Queensland and New South Wales (Fig. 17), producing most of the highest daily rainfall totals of the summer (Table 1). Although 2012–13 was below average for the number of tropical cyclone formations, four tropical cyclones significantly affected the Australian region in summer 2012–13. Three of these, tropical cyclone *Oswald*, tropical cyclone *Peta* in January and severe tropical cyclone *Rusty* in February made landfall in Australia, and a fourth, severe tropical cyclone *Narelle*, stayed offshore but affected northern Western Australia. Although a relatively weak category 1 storm, tropical cyclone *Oswald* produced heavy rainfall and major flooding at the end of January 2013 after it crossed the northern Queensland coast several times between 19 and 22 January and then tracked southwards for several days just inland from the Queensland coast (see Special Climate Statement 44, Bureau of Meteorology 2013a). Tropical cyclone *Oswald* produced exceptional daily rainfall totals including 653.0 mm at Numinbah in Queensland and 444.0 mm at Chillingham in New South Wales on 28 January (Table 1) and broke numerous single- and multi-day rainfall

Fig. 16. Summer 2012–13 rainfall totals (mm) for Australia.

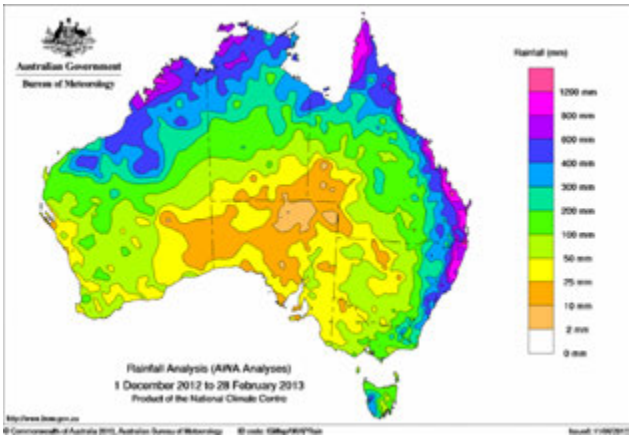

Fig. 17. Summer 2012–13 rainfall deciles for Australia.

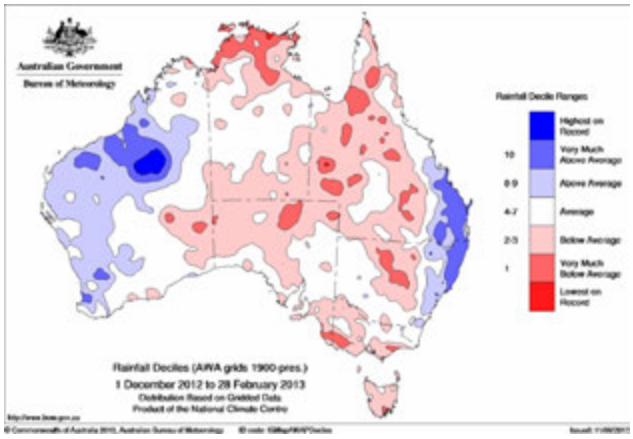

Fig. 18. Summer 2012–13 maximum temperature anomalies (°C).

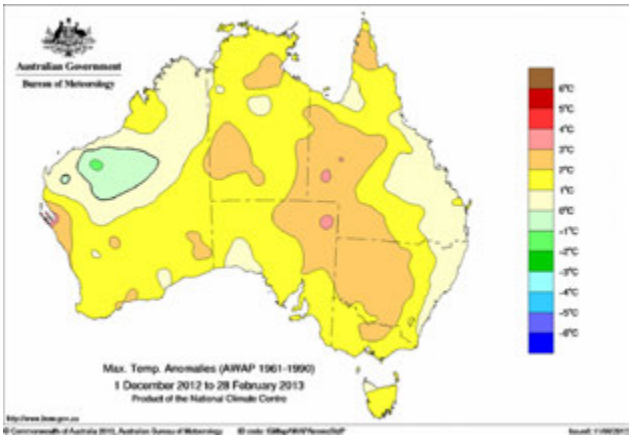

Fig. 19. Summer 2012–13 maximum temperature deciles.

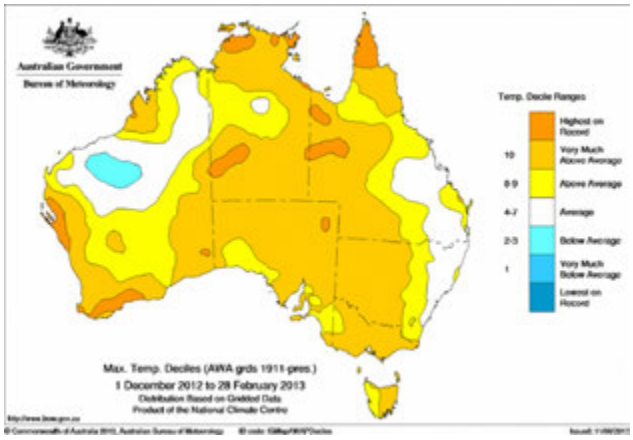

Fig. 20. Summer 2012–13 minimum temperature anomalies (°C).

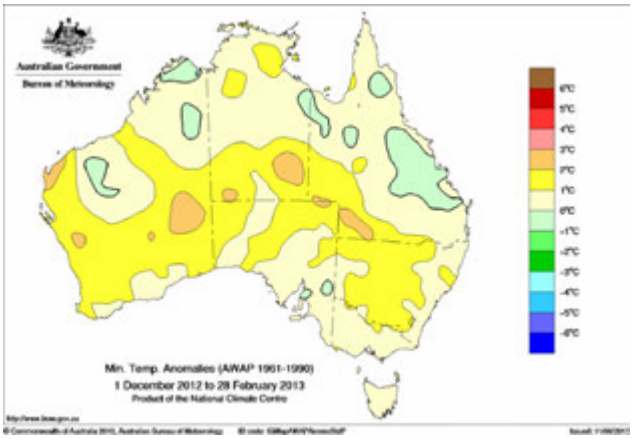

Fig. 21. Summer 2012–13 minimum temperature deciles.

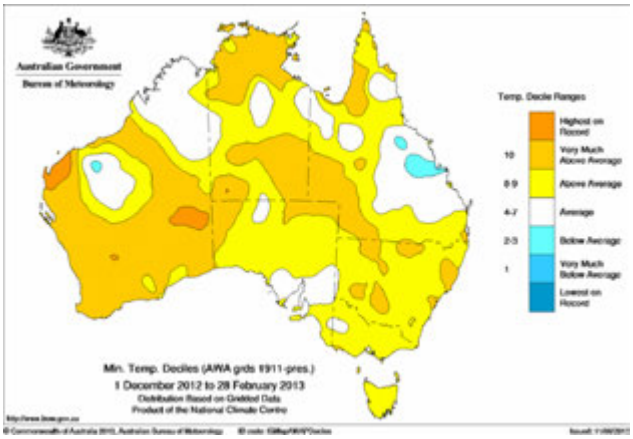

*Figures 16 to 21 produced by the National Climate Centre, Australian Bureau of Meteorology using the Australian Water Availability Project (AWAP) analysis (Jones et al. 2009). Anomalies are with respect to a 1961–1990 normal. For stations with insufficient data within this period, a normal was estimated using gridded climatologies. Decile ranges are based on grid-point values over the summers 1911–12 to 2011–12 (temperature) or 1900–01 to 2011–12 (rainfall).

Table 1. Summary of the seasonal rainfall ranks and extremes on a national and State basis for summer 2012–13. The ranking in the 2nd last column goes from 1 (lowest) to 113 (highest) and is calculated over the years 1900–2012.

Region	*Highest seasonal total (mm)*	*Lowest seasonal total (mm)*	*Highest daily total (mm)*	*Area-averaged rainfall (mm)*	*Rank of area-averaged rainfall*	*% difference from mean*
Australia	2200.0 at Springbrook TM (QLD)	0.0 at Macumba (SA)	653.0 at Numinbah (QLD), 28 January	180	36	–13%
Queensland	2200.0 at Springbrook TM	8.6 at Bedourie Police Station	653.0 at Numinbah, 28 January	259	28	–20%
New South Wales	1792.8 at Yarras (Mount Seaview)	11.5 at Hungerford (Willara)	444.0 at Chillingham (Limpinwood), 28 January	166	68	–3%
Victoria	341.8 at Mount Hotham	11.0 at Nulkwyne Kiamal	136.0 at Dellicknora, 29 January	84	28	–29%
Tasmania	603.8 at Mount Read*	49.9 at Hobart Botanical Gardens	69.0 at Wynyard Airport, 15 December	184	20	–24%
South Australia	105.6 at Peterborough	0.0 at Macumba	58.0 at Peterborough (Amelia), 22 February	25	17	–59%
Western Australia	949.8 at Country Downs	12.4 at Sandsprings	263.4 at Bamboo Creek, 28 February	178	87	+20%
Northern Territory	932.4 at Geriatric Park	7.0 at Andado	170.6 at Berrimah Research Farm, 12 February	222	18	–30%

*Four days missing data.

Table 2. Percentage areas in different categories for summer 2012–13 rainfall. 'Severe deficiency' denotes rainfall at or below the 5th percentile. Areas in 'decile 1' include those in 'severe deficiency', which in turn include those which are 'lowest on record'. Areas in 'decile 10' include those which are 'highest on record'. Percentage areas of highest and lowest on record are given to two decimal places because of the small quantities involved; other percentage areas to one decimal place.

Region	*Lowest on record*	*Severe deficiency*	*Decile 1*	*Decile 10*	*Highest on record*
Australia	0.15	2.0	7.4	6.2	0.77
Queensland	0.16	3.4	13.3	6.9	0.04
New South Wales	0.00	1.1	7.1	8.3	0.16
Victoria	1.07	4.8	12.6	0.0	0.00
Tasmania	0.00	0.0	7.1	0.0	0.00
South Australia	0.00	1.2	7.3	0.0	0.00
Western Australia	0.00	0.0	1.0	11.3	2.29
Northern Territory	0.46	4.8	11.2	0.0	0.00

records across the region (Special Climate Statement 44, Bureau of Meteorology 2013a). Tropical cyclone *Oswald* caused widespread flooding across Queensland and New South Wales, most notably in the Burnett catchment in Queensland and the Clarence catchment in northern New South Wales, both of which reached record flood peaks. Tropical cyclone *Oswald* also created coastal storm surges and high waves, as well as a number of tornadoes, particularly in the Bundaberg area. A storm surge of around 0.5 m above normal tide levels was observed at several points along the Queensland and New South Wales coast, with 0.59 m observed at Tweed Heads, while offshore waves exceeding 12 m were observed off Coffs Harbour. Significant coastal erosion and some inundation of foreshore areas were also experienced.

Severe tropical cyclone *Narelle*, tropical cyclone *Peta* and severe tropical cyclone *Rusty* contributed to the higher than normal rainfall totals in Western Australia during summer 2012–13 (Fig. 17). Although it did not make landfall in Australia, category 4 severe tropical cyclone *Narelle* produced thunderstorms across Western Australia as it tracked southwards approximately 300 km off the northern Western Australia coastline in early January, and pushed moist air into South Australia, providing some rainfall relief to the region. Category 1 tropical cyclone *Peta* made landfall on 23 January along the Pilbara coastline in Western Australia, and produced heavy rainfall and flooding in the region. Category 4 severe tropical cyclone *Rusty* had the biggest impact on Western Australia in summer 2012–13. A very slow moving system, severe tropical cyclone *Rusty* made landfall on 27 February approximately 100 km east of Port Hedland and produced high winds and heavy rainfall

Table 3. Summary of the seasonal maximum temperature ranks and extremes on a national and State basis for summer 2012–13. The ranking in the last column goes from 1 (lowest) to 103 (highest) and is calculated over the years 1910–2012†.

Region	*Highest seasonal mean maximum (°C)*	*Lowest seasonal mean maximum (°C)*	*Highest daily maximum temperature (°C)*	*Lowest daily maximum temperature (°C)*	*Area-averaged temperature anomaly (°C)*	*Rank of area-averaged temperature anomaly*
Australia	41.4 at Urandangi Aerodrome (QLD)	13.9 at Mount Wellington (TAS)	49.6 at Moomba (SA), 12 January	–0.2 at Mount Baw Baw (VIC), 4 December	+1.44	103
Queensland	41.4 at Urandangi Aerodrome	26.4 at Applethorpe	49.0 at Birdsville, 13 January	19.7 at Toowoomba, 25 February	+1.58	100
New South Wales	37.8 at Wanaaring	16.6 at Thredbo (Top Station)	48.6 at Wanaaring, 12 January	3.0 at Charlotte Pass, 28 February	+1.90	97
Victoria	33.8 at Mildura	16.2 at Mount Hotham	45.7 at Yarrawonga, 5 January	–0.2 at Mount Baw Baw, 4 December	+1.77	100
Tasmania	25.3 at Cressy	13.9 at Mount Wellington	41.8 at Hobart, 4 January	2.4 at Mount Wellington, 4 December	+1.09	90
South Australia	39.8 at Moomba	22.6 at Cape Willoughby	49.6 at Moomba, 12 January	13.9 at Mount Lofty, 3 December	+1.98	102
Western Australia	40.5 at Emu Creek	23.5 at Albany	49.0 at Leonora, 9 January	16.6 at Mount Barker, 12 December	+0.95	94
Northern Territory	40.5 at Walungurru	32.2 at McCluer Island	46.7 at Walungurru, 9 January and at Rabbit Flat, 25 January	21.3 at Kulgera, 28 February	+1.44	102

Table 4. Summary of the seasonal minimum temperature ranks and extremes on a national and State basis for summer 2012–13. The ranking in the last column goes from 1 (lowest) to 103 (highest) and is calculated over the years 1910–2012†.

Region	*Highest seasonal mean minimum (°C)*	*Lowest seasonal mean minimum (°C)*	*Highest daily minimum temperature (°C)*	*Lowest daily minimum temperature (°C)*	*Area-averaged temperature anomaly (°C)*	*Rank of area-averaged temperature anomaly*
Australia	27.6 at Centre Island (NT)	4.7 at Mount Wellington (TAS)	34.1 at Bedourie (QLD), 14 January	–5.3 at Perisher Valley (NSW), 10 December	+0.79	98
Queensland	27.3 at Sweers Island	15.3 at Applethorpe	34.1 at Bedourie, 14 January	5.5 at Stanthorpe, 6 December	+0.61	93
New South Wales	22.9 at Tibooburra Post Office	6.1 at Perisher Valley	32.2 at Broken Hill Airport and Pooncarie and Tibooburra, 18 January	–5.3 at Perisher Valley, 10 December	+1.31	95
Victoria	16.8 at Mildura	7.2 at Mount Baw Baw	29.0 at Echuca, 5 January	–3.7 at Dinner Plain, 10 December	+0.90	88 (tied)
Tasmania	14.7 at Swan Island	4.7 at Mount Wellington	23.4 at Hobart, 4 January	–2.7 at Mount Wellington, 5 December	+0.51	85 (tied)
South Australia	23.6 at Moomba	11.3 at Naracoorte	32.4 at Arkaroola, 18 January	11.3 at Naracoorte, 10 December	+0.96	90
Western Australia	27.5 at Varanus Island	13.1 at Rocky Gulley	33.5 at Wiluna, 9 January	3.8 at Wandering, 1 December and at Eyre, 30 January	+0.78	99
Northern Territory	27.6 at Centre Island	21.1 at Alice Springs	32.8 at Walungurru, 22 January	12.0 at Kulgera, 02 February	+0.58	94 (tied)

†The Australian Climate Observations Reference Network – Surface Air Temperature (ACORN-SAT) dataset (Trewin 2012) is used to calculate the spatial averages and rankings shown in Table 3 (maximum temperature) and Table 4 (minimum temperature). These averages are available from 1910 to the present.

Table 5. Percentage areas in different categories for summer 2012–13 temperature. Areas in 'decile 1' include those which are 'lowest on record'. Areas in 'decile 10' include those which are 'highest on record'. Percentage areas of highest and lowest on record are given to two decimal places because of the small quantities involved; other percentage areas to one decimal place. Grid-point deciles calculated with respect to 1911–2012.

Region	*Maximum temperature*				*Minimum temperature*			
	Lowest on record	*Decile 1*	*Decile 10*	*Highest on record*	*Lowest on record*	*Decile 1*	*Decile 10*	*Highest on record*
Australia	0.00	0.00	58.80	5.34	0.00	0.00	39.40	1.47
Queensland	0.00	0.00	55.80	8.47	0.00	0.00	22.30	0.00
New South Wales	0.00	0.00	60.70	0.00	0.00	0.00	24.60	0.00
Victoria	0.00	0.00	92.10	0.00	0.00	0.00	0.80	0.00
Tasmania	0.00	0.00	62.20	0.00	0.00	0.00	0.00	0.00
South Australia	0.00	0.00	87.20	0.90	0.00	0.00	19.40	0.00
Western Australia	0.00	0.00	35.80	5.10	0.00	0.00	61.60	4.45
Northern Territory	0.00	0.00	77.50	9.53	0.00	0.00	52.80	0.11

over a prolonged period primarily over the Pilbara region, including the State's highest daily total for the summer of 263.4 mm at Bamboo Creek on 28 February.

A summary of the rainfall ranks and extremes are shown in Table 1 for each State and Territory, with corresponding rainfall deciles (e.g. highest and lowest on record) provided in Table 2.

Drought

Below average rainfall between March and November 2012 across many parts of southern Australia caused short-term rainfall deficiencies in many regions, including southwestern and eastern Western Australia and much of South Australia (not shown). While summer 2012–13 rainfall totals eased the deficiencies in some regions (Table 2)—notably in southwest Western Australia—all States and Territories exhibited some areas with totals in the lowest ten per cent of rainfall records (serious deficiency), with all except Western Australia and Tasmania experiencing rainfall in the lowest five per cent of records (severe deficiency). Nationally, 7.4 per cent of Australia experienced serious deficiency, with two per cent severe deficiency. Victoria and the Northern Territory were particularly dry with 12.6 per cent and 11.2 per cent experiencing serious deficiency, 4.8 per cent and 4.8 per cent severe deficiency and 1.07 per cent and 0.46 per cent the lowest on record respectively. In contrast, 11.3 per cent of Western Australia experienced rainfall in the highest ten per cent of records (very much above average) and 2.29 per cent the highest on record.

Temperature

Summer 2012–13 saw large parts of central and southern Australia impacted by persistent and widespread extreme maximum temperatures. Following an abnormally hot spring 2012, particularly for daily maximum temperatures (Reid 2013), and one of the most significant spring heatwaves on record that affected large parts of eastern Australia in the last week of November 2012 (see Special Climate Statement 41, Bureau of Meteorology 2012b), the unusually hot conditions across Australia continued into summer 2012–13. This extended period of extreme heat was exacerbated by dry conditions, which had been affecting much of Australia since the middle of 2012 (Pepler 2013, Reid 2013), and a delayed start to a weak Australian monsoon. Late December 2012 to mid-January 2013, in particular, observed a significant widespread heatwave event that affected most parts of the country, with many temperature records approached or broken across southern and central Australia (see Special Climate Statement 43, Bureau of Meteorology 2013b). The heatwave event commenced with a build up of extreme heat in southwestern Western Australia at the end of December 2012, as a high in the Bight and a trough near the west coast directed hot easterly winds over the region. From 31 December, the high pressure system shifted eastwards, bringing well above average temperatures across southern Western Australia. By 4 January 2013, the high pressure system had moved off eastern Australia, with northerly winds directing very hot air into the southeastern mainland and Tasmania, before the area of intense heat moved northeast as the high pressure system centred over the Tasman Sea and a low pressure trough directed hot northerly winds into western New South Wales and South Australia in the second week in January.

When averaged across Australia, maximum temperatures for summer 2012–13 were 1.44 °C above average, making it the warmest Australian summer on record based on observations since 1910–11 (Table 3). Individually, each State and Territory observed maximum area-averaged temperature anomalies greater than or equal to 0.95 °C for the summer, with New South Wales (1.90 °C, ranked 7th warmest) and South Australia (1.98 °C, ranked 2nd warmest) recording the highest anomalies (Table 3). South Australia also observed the highest daily maximum temperature in the country with 49.6 °C recorded at Moomba Airport on 12 January. All States and Territories observed their highest daily maximum values during January, corresponding with the persistent heatwave event that affected most of the country. Queensland and Tasmania recorded their second

highest area-averaged daily maximum temperatures, with Hobart observing its highest daily maximum temperature from 130 years of record (41.8 °C) on 4 January, breaking the previous record by 1.0 °C which is exceptional. The record temperatures in Tasmania also corresponded with bushfires in the southeast of the State. The lowest daily maximum temperature was –0.2 at Mount Baw Baw in Victoria on 4 December. Figure 18 shows the maximum temperature anomalies for summer 2012–13, relative to a reference period of 1961–1990. There was limited variation across the country with positive maximum temperature anomalies observed across almost all of the country, with the exception being a region in northwestern Western Australia. This is reflected in the maximum temperature deciles for the summer (Fig. 19, Table 5), calculated using monthly maximum temperatures from 1911 to 2012, showing the majority of Australia observed very much above average maximum temperatures, and in some regions highest on record temperatures. The exception was average to below average maximum temperature deciles observed across northwestern Western Australia and over parts of eastern Australia, which are well correlated with the above average to very much above average rainfall deciles observed in these regions during the summer (see earlier section).

Minimum temperatures were also exceptionally high during summer 2012–13. When averaged across the whole of Australia, minimum temperatures were 0.79 °C above average, ranking 6th warmest on record (Table 4). Similar to maximum temperatures, the high minimum temperatures were widespread. There was limited variability across the country (Fig. 20) with most regions seeing positive minimum temperature anomalies relative to a reference period of 1961–1990, and only limited areas across the northern half of the country observing negative anomalies. Each State and Territory observed positive minimum area-averaged temperature anomalies, with the highest anomaly in New South Wales (1.31 °C) and the lowest in Tasmania (0.51 °C) for the summer (Table 4). As with maximum temperatures, all States and Territories observed their highest daily minimum values during January. The minimum temperature deciles for the summer (Fig. 21, Table 5) show the majority of Australia observed above average minimum temperatures, and in some regions—notably central Australia and Western Australia—very much above average minimum temperatures. Exceptions were average to below average minimum temperature deciles observed across northeastern Queensland and parts of northern Western Australia. Of the highest daily minimum temperature recorded over the summer (Table 4), the highest was 34.1 °C, recorded at Bedourie in Queensland on 14 January. The lowest was 23.4 °C recorded at Hobart in Tasmania on 4 January, although this was Hobart's hottest January minimum on record.

A summary of the maximum and minimum temperature ranks and extremes for each State and Territory are provided in Tables 3 and 4 respectively, with corresponding maximum and minimum temperature deciles given in Table 5.

Acknowledgments

The authors wish to thank Lorien Martin, Phillip Reid and Mike Pook for their assistance with some of the datasets and for providing comments and advice on earlier drafts of this paper.

References

Bureau of Meteorology. 2012a. Very heavy December rainfall in southwest Western Australia. *Special Climate Statement 42*, Bureau of Meteorology, Australia. Accessible via www.bom.gov.au/climate/current/special-statements.shtml

Bureau of Meteorology. 2012b. Extreme November heat in eastern Australia. *Special Climate Statement 41*, Bureau of Meteorology, Australia. Accessible via www.bom.gov.au/climate/current/special-statements.shtml

Bureau of Meteorology. 2013a. Extreme rainfall and flooding in coastal Queensland and New South Wales. *Special Climate Statement 44*, Bureau of Meteorology, Australia. Accessible via www.bom.gov.au/climate/current/special-statements.shtml

Bureau of Meteorology. 2013b. Extreme January heat. *Special Climate Statement 43*, Bureau of Meteorology, Australia. Accessible via www.bom.gov.au/climate/current/special-statements.shtml

Donald, A., Meinke, H., Power, B., Maia, A.H.N., Wheeler, M.C., White, N., Stone, R.C. and Ribbe. J. 2006. Near-global impact of the Madden-Julian Oscillation on rainfall. *Geophys. Res. Lett., 33,* L09704.

Hoerling, M.P., Kumar, A., Zhong, M. 1997. El Niño, La Niña, and the Nonlinearity of Their Teleconnections. *J. Clim., 10,* 1769–86.

Imielska, A. 2011. Seasonal climate summary southern hemisphere (summer 2010–2011): second wettest Australian summer on record and one of the strongest La Niña events on record. *Aust. Met. Oceanogr. J., 61,* 241–51.

Jones, D.A., Wang, W. and Fawcett, R.J. 2009. High-quality spatial climate datasets for Australia. *Aust. Met. Oceanogr. J., 58,* 233–48.

Kuleshov, Y., Qi, L., Fawcett, R. and Jones, D. 2009. 'Improving preparedness to natural hazards: Tropical cyclone prediction for the southern hemisphere,' in: Gan, J. (Ed.), *Advances in Geosciences, Vol. 12 Ocean Science*, World Scientific Publishing, Singapore, 127–43.

Martin, L. 2013. Seasonal climate summary southern hemisphere (autumn 2012): the transition from La Niña to neutral. *Aust. Met. Oceanogr. J., 63,* 249–59.

Pepler, A. 2013. Seasonal climate summary southern hemisphere (winter 2012): Dry conditions return to Australia. Submitted to *Aust. Met. Oceanogr. J., 63,* 339–49.

Reid, P. 2013. Seasonal climate summary southern hemisphere (spring 2012): warmer and dryer across much of Australia and a new southern hemisphere sea ice extent record. *Aust. Met. Oceanogr. J., 63,* 427–42..

Risbey, J.S., Pook, M.J., McIntosh, P.C., Wheeler, M.C. and Hendon, H.H. 2009. On the remote drivers of rainfall variability in Australia. *Mon. Weather Rev., 137,* 3233–53.

Trewin, B.C. 2012. Techniques involved in developing the Australian Climate Observations Reference Network – Surface Air Temperature (ACORN-SAT) dataset. CAWCR Technical Report No. 49.

Troup, A.J. 1965. The Southern Oscillation. *Q. J. R. Meteorol. Soc., 91,* 490–506.

Webb, M. 2013. Seasonal climate summary southern hemisphere (summer 2011–12): a mature La Niña, strongly positive SAM and active MJO. *Aust. Met. Oceanogr. J., 62,* 335–49.

Wheeler, M.C. and Hendon, H.H. 2004. An all-season real-time multivariate MJO Index: Development of an index for monitoring and prediction. *Mon. Weath. Rev., 132,* 1917–32.

Wheeler, M.C., Hendon, H.H., Cleland, S., Meinke, H. and Donald, A. 2009: Impacts of the Madden-Julian oscillation on Australian rainfall and circulation. *J. Clim., 22,* 1482–98.

Wolter, K. and Timlin, M.S. 1993. Monitoring ENSO in COADS with a seasonally adjusted principal component index. Proc. Of the 17th Climate Diagnostics Workshop, Norman, OK, NOAA/NMC/CAC, NSSL, Oklahoma Clim. Survey, CIMMS and the School of Meteorology, Univ. of

Oklahoma, 52–7.

Wolter, K. and Timlin, M.S. 1998. Measuring the strength of ENSO – how does 1997/98 rank? *Weather, 53,* 315–24.

Zhang, C. 2005. Madden–Julian Oscillation. *Rev. Geophys., 43,* RG2003, 36pp, doi:10.1029/2004RG000158.